Supplementary for Reconstructing the ocean's mesopelagic zone carbon budget: sensitivity and estimation of parameters associated with prokaryotic remineralization

A)

Table S1: Parameter definition from Anderson & Tang 2010 model. Values are shown for the cases where parameters were set in the optimization procedure. These values are from the parametrization used in both Anderson & Tang 2010 and Giering et al. 2014

Description	Parameter	Value
Proportion of sinking POC taken by sinking prokaryotes	Ψ	not fixed
Losses of DOC solubilized by sinking prokaryotes	α	not fixed
Sinking prokaryotes'PGE	ω_a	not fixed
Non-sinking prokaryotes' PGE	ω_{fl}	not fixed
Losses of DOC by sinking prokaryotes consumers	Φv	0.05
Sinking prokaryotes consumers absorption efficiency	βv	0.72
Sinking prokaryotes consumers net growth efficiency	Kv	0.44
Losses of DOC excreted by non-sinking prokaryotes consumers	Φv	0.05
Non-sinking prokaryotes consumers absorption efficiency	βv	0.72
Non-sinking prokaryotes consumers net growth efficiency	Kv	0.44
Losses of DOC excreted by non-sinking prokaryotes	Φz	0.05
Carnivores absorption efficiency	βz	0.66
Losses of suspended POC by carnivrores sloppy feeding	λz	0.15
Carnivores net growth efficiency	Kz	0.39
Losses of DOC by detritivores excretion	Φh	0.05
Detritivores absorption efficiency	βh	0.60
Losses of suspended POC by detritivores sloppy feeding	λh	0.30
Detritivores net growth efficiency	Kh	0.39
Proportion of prokaryotes taken by prokaryotes consumers	ζ	0.48
Proportion of prokaryotes consumers taken by detritivores	ζ2	0.48

B)

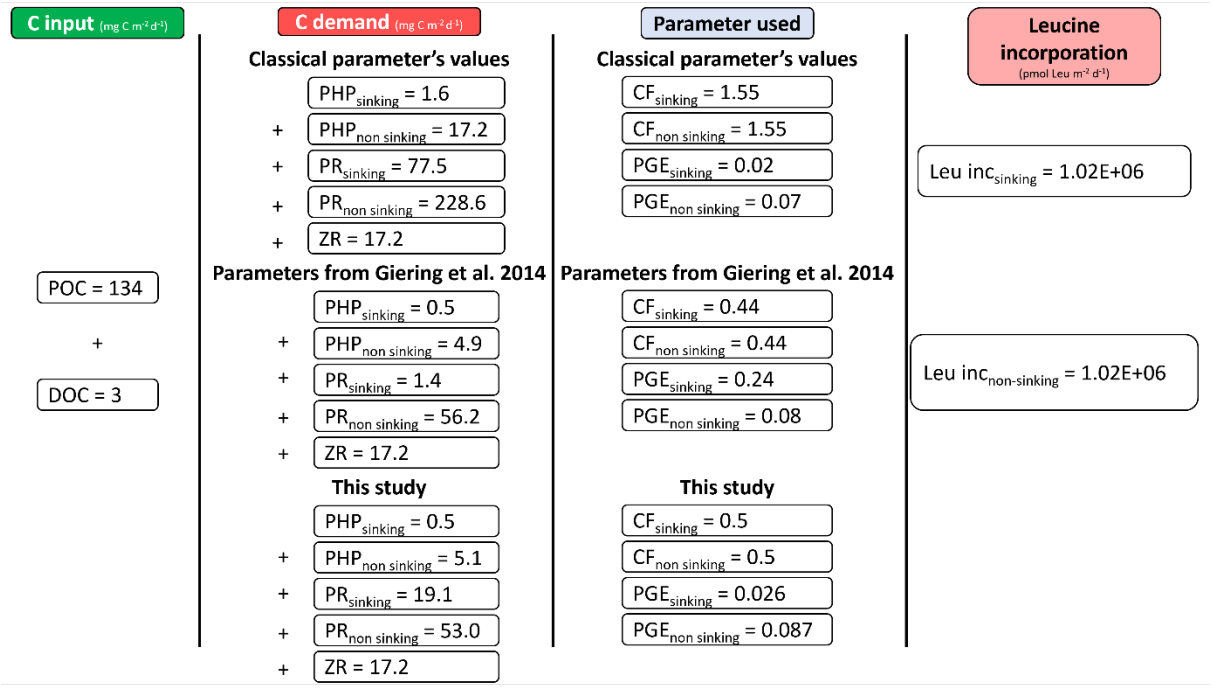

Figure S1: *Integrated carbon budget for the active mesopelagic zone estimation resulting from DY032 measurements or estimation. Different combinations of CF,* $PGE_{sinking}$ *and* $PGE_{non\text{-}sinking}$ *were applied on leucine incorporation rates of sinking and non-sinking prokaryotes. These values correspond to the Figure 1 of the main manuscript*

C)

Attempts to calculate α parameter from Anderson & Tang model using the PEACETIME dataset

- **For total hydrolyzable carbohydrates (TCHO)** > 1 kDa samples, pre-combusted glass vials (8 h, 500°C) were filled with 20 ml of seawater for each duplicate, which was then kept at -20 °C until analysis. According to Engel and Händel, (2011), samples were hydrolyzed for 20 h at 100°C with 0.8 M HCl final concentration with subsequent neutralization using acid evaporation (N2, for 5 h at 50°C). TCHO were analyzed using a Dionex ICS 3000 ion chromatography system equipped with high-performance anion exchange chromatography with pulsed amperometric detection (HPAEC-PAD).
- **Total hydrolyzable amino acids (TAA)** were measured from a duplicate of 5 mL of sample which was filled into pre-combusted glass vials (8 h, 500°C) and stored at -20°C. Analysis was performed according to Lindroth and Mopper (1979) and Dittmar et al.

(2009) with some modifications. The samples were hydrolyzed at 100°C for 20 h with 1 mL 30% HCl (Suprapur® , Merck) to 1 ml of sample added and neutralized by acid evaporation under vacuum at 60°C in a microwave. Remaining acid was removed with water. Total hydrolyzable amino acids analysis were performed by high-performance liquid chromatography (HPLC) using an Agilent 1260 HPLC system following a modified version of established methods (Lindroth and Mopper, 1979; Dittmar et al., 2009).

- **Ecto-enzymatic activities:** Fluorogenic model substrates L-leucine-7-amido-4-methyl-coumarin (Leu-MCA) and 4 methylumbelliferyl-D-glucopyranoside (MUF-glu) were used to evaluate the ectoenzymatic activities of aminopeptidase (LAP) and b-glucosidase (GLU), respectively (Hoppe, 1983). Briefly, in a 24-wells black polystyrene plate, 2 mL of seawater samples were combined in triplicate with 100 L of a fluorogenic substrate with a final concentration of 500 nM. Aminopeptidase activity and b-glucosidase activity were incubated at *in situ* temperature and followed by measuring increase of fluorescence (exc/em 380/440 nm for MCA and 365/450 nm for MUF, wavelength width 5 nm) in a VARIOSCAN LUX microplate reader (Van Wambeke et al. 2020).

- **Conversion into hydrolyzed C fluxes:**
Michaelis-Menten function is defined as V=Vm x S/(Km+S), with V the hydrolysis rate in nmol of amino acids hydrolyzed l^{-1} h^{-1} , Vm the maximum hydrolysis velocity, Km the Michaelis–Menten half-saturation constant and S the substrate concentration (we assume that S = 500 nM corresponds to the initial rate). As ecto-enzymatic activities were measured using only one substrate concentration, we are not able to determine Km. Thus, we used the same method as Hoppe et al. (1993) using the turnover rate V/S = Vm/Km in h^{-1} which we multiply by real substrate concentration (cf below for specific cases of each enzyme). Using such a method, we may overestimate the real hydrolysis rate. However, in cases of particles where the substrate is supposed to be locally highly concentrated around attached prokaryotes, we could expect that their enzymatic gear is adapted to high substrate concentrations and thus with Km comparable to the "Km_{all}" from the upper range of non-sinking prokaryotes in the same cruise and stations (Van Wambeke et al. 2021). In that case, S is negligible regarding Km and V ≈ Vm x S/Km.

Case of MCA-Leu aminopeptidase:

The artificial substrate used to measure the activity was only leucine which contains 6 mol of C per amino acid. For other amino acids this is not necessarily the case. We multiply THAA concentration in nmol L^{-1} of each amino acid by the corresponding number of C atoms and sum all to obtain total amino acid C concentration. We are thus able to calculate the 'true velocity' equal to (V/S) x [amino acid C].

Case of MUF β-glucosidase:

We suppose that sugar constitutes the substrate of β-glucosidase. We multiply TCHOO concentration in nmol L^{-1} of each sugar with the corresponding number of C atoms and then sum up all to obtain total sugar C concentration. We are thus able to calculate the real hydrolysis rate equal to (V/S) x [sugar C].

Results:

Station	Depth	Total amino acids C concentration (nmol C L^{-1})	Total sugar C concentration (nmol C L^{-1})	C hydrolised by MCA-Leu aminopeptidase (mg C $m^{-3}d^{-1}$)	C hydrolised by MUF βglucosidase (mg C $m^{-3}d^{-1}$)	Total hydrolised C (mg C $m^{-3}d^{-1}$)	Hydrolyzed C released (mg C $m^{-3}d^{-1}$)	α
TYR	**70**	10.37	62.96	1.96E-05	6.00E-05	7.96E-05	-1.75E-04	NA
TYR	**80**	3.17	189.06	5.81E-06	1.18E-05	1.76E-05	1.39E-05	78.68
TYR	**90**	3.31	51.32	NA	NA	0.00E+00	-7.06E-05	NA
TYR	**200**	9.81	244.89	6.20E-07	4.82E-06	5.44E-06	1.31E-06	23.99
ION	**80**	3.00	3.49	3.15E-07	1.21E-07	4.36E-07	-2.20E-06	NA
ION	**100**	1.40	1.25	9.76E-08	2.23E-07	3.20E-07	-8.90E-06	NA
ION	**150**	06.03	1.95	3.44E-07	4.95E-08	3.94E-07	-1.05E-04	NA
ION	**200**	7.00	535.52	2.64E-07	1.08E-04	1.08E-04	5.03E-05	46.54
FAST	**80**	8.89	7.15	3.16E-05	1.22E-06	3.29E-05	1.20E-05	36.46
FAST	**70**	14.19	29.91	NA	NA	0.00E+00	-1.27E-04	NA
FAST	**75**	8.99	15.91	2.20E-05	4.44E-07	2.24E-05	-5.37E-04	NA
FAST	**100**	67.67	19.18	1.98E-04	4.42E-05	2.42E-04	4.61E-05	19.06

D)

Table S2 Methods to measure prokaryotic respiration: general characteristics

Methods	Pros and cons and Features	Fraction targeted	Sources
Direct measurements of O_2 consumption (or CO_2 production) by titration or measurements of DOC concentration decrease	Assumes a constant and fixed O_2 consumption/CO_2 production stoichiometry and not sensitive enough for deep samples	Neutrally buoyant particles and DOC	(Burd et al. 2010)
Electron Transport System (ETS). This method estimates the potential activity (Vmax) of enzymes associated with the respiratory chains	Commonly used method, no difference between eukaryotes and prokaryotes, measures with under-saturated substrates, it is more a matter of a maximum respiration rate rather than real	Neutrally buoyant particles and DOC	(e.g. Packard et al. 1988; Robinson 2019)
Measurements of $^{14}CO_2$ production during incubations with ^{14}C labeled components	difficulty in picking the 'ideal' substrate (e.g. ^{14}C-glutamate)	DOC	(e.g. Tamburini et al. 2003)
Measurement with polarographic probe	The probe has its own O_2 consumption which can produce a bias, High-frequency measurements	DOC & particles	(Langdon 1984)
Measurements with Optode	Easy to use, high-frequency measurements, clogs easily. *In situ* rates are found higher than expected (see discussion)	Neutrally buoyant particles and DOC	(Tengberg et al. 2006)
Measurements with O_2 microelectrode	Single particle measurements, Use of a model to convert O_2 concentration into a flux in any particles. The particles are kept in suspension by a continuous flow during the measurements	Single particles	(Ploug and Jorgensen 1999; Iversen et al. 2010)
RESPIRE	I*n situ* measurement of O_2 consumption after incubation of trapped particles, use an Optode (see Optode above)	Sinking particles	(Boyd et al. 2015)
PHORCYS, AutoBOD	Incubation of 70h, maximum depth of 100m, use an Optode (see Optode above), incubation are done in both, opaque and transparent chambers	All fractions	(Van Mooy and Keil 2015; Collins et al. 2018)

$IODA_{6000}$	Incubation of 5-days, maximum depth of 6000m, use an Optode (see Optode above)	Neutrally buoyant particles and DOC	(Robert 2012)
Estimation from Prokaryotic Growth Efficiency (PGE) and PHP	Results depending on the choice of a PGE value and a conversion factor Thymidine/Carbon or Leucine/Carbon	All fractions if PHP are measured	(del Giorgio and Cole 1998)

E)

Table S3: Parameter estimations and associated output flux errors obtained from model inversion without accounting for zooplankton respiration flux. The estimation corresponds to the median estimation over 100 runs and 90% confidence intervals are given in brackets.

Estimation	Estimation	Estimation	Estimation	Error	Error	Error
Ψ	**$PGE_{sinking}$**	**$PGE_{non-sinking}$**	**α**	**$PHP_{non-sinking}$**	**$PHP_{sinking}$**	**$PR_{sinking}$**
0.675 (0.438 ; 0.989)	0.026 (0.026 ; 0.026)	0.088 (0.077 ; 0.100)	0.774 (0.685 ; 0.831)	0.084 %	0.370 %	0.032%

Table S4: Parameter estimations and associated loss (as detailed in equation (1)) obtained using different experimental settings. Confidence intervals are not given for concision. When bounded, PGEs cannot exceed 0.1.

	$CF_{non-sinking}$ = 1.55, PGEs bounded	$CF_{non-sinking}$ = 0.5, PGEs bounded	CFs=1.55, PGEs bounded	CFs=0.5, PGEs bounded	CFs unfixed, PGEs bounded	CFs unfixed, PGEs not bounded
Ψ	0.734	0.696	0.727	0.675	0.706	0.951
$PGE_{sinking}$	0.099	0.093	0.080	0.026	0.090	0.173
$PGE_{non-sinking}$	0.100	0.087	0.100	0.087	0.097	0.226
α	0.786	0.767	0.790	0.777	0.769	0.795
$CF_{sinking}$	1.956	1.934	1.55	0.500	1.865	3.927

$CF_{non\text{-}sinking}$	1.55	0.500	1.55	0.500	0.563	1.526
loss	0.621	0.000	0.621	0.000	0.000	0.000

Table S5: Uncertainty analysis: impact of simulated errors in measurement of the main fluxes used to estimate the parameters. The table presents the coefficients of variation (CV, %) for each parameter associated with perturbations of the measured fluxes (namely: Net POC input, DOC input, heterotrophic production (PHP) of sinking and non-sinking prokaryotes, and respiration (PR) of sinking prokaryotes and respiration of the zooplankton) by +- 10% over 10 runs each.

Flux with simulated measurement error/induced change in the parameter (%)	**Ψ**	**$PGE_{sinking}$**	**$PGE_{non\text{-}sinking}$**	**α**
Net POC input	2.09	0.01	6.26	1.9
DOC input	0.02	1.11	4.57	0.32
Non-sinking prokaryotes PHP	0.84	0	5.41	0.2
Sinking prokaryotes PHP	0.06	6.23	0	0.03
Sinking prokaryotes PR	0.01	6.26	1.38	1.81
Zooplankton respiration	3.08	0	0.99	0.68

F)

Depth profile of non-sinking prokaryotes heterotrophic activities under *in situ* hydrostatic pressure

Samples were collected at depths of 250, 400, 1000 and 2500m using the pressure-retaining sampler described in Garel et al. 2019. This device is specifically designed to keep the *in situ* pressure of the sample using High Pressure Sampler Unit (HPSU). Samples were then transferred under equipressure for samples kept under *in situ* pressure, or at atmospheric pressure for depressurized controls into 3 independent High Pressure Bottles (HPBs) (triplicate), previously amended with L-[4,5-^{3}H]-Leucine (^{3}H-Leu with a specific activity of

109 Ci $mmol^{-1}$, PerkinElmer®) at final concentration of 10 nM. After 10h of incubation, samples were processed as in Garel et al. (2019).

In parallel, the leftover volume from the HPSU is used to measure dissolved-oxygen consumption using optic fiber and planar optodes (Presens GmbH Pst3), glued on sapphire windows included in HPBs (see Garel et al 2019 for details). Optic fibers were plugged to the OXY-10 mini device (from Presens GmbH) used as the data logger. The optodes were previously calibrated manually using a two-point calibration procedure and pre-conditioned at the pressure of incubation. Temperature was recorded throughout the incubation period using PT100. Data are then compensated from the hydrostatic pressure, temperature and salinity using algorithms proposed by McNeil and D'Asaro (2014).

Respiration rates were calculated using a constant RQ of 1 and as we demonstrate in the paper that universal use of parameters is not necessarily adequate, these results should be taken with special care.

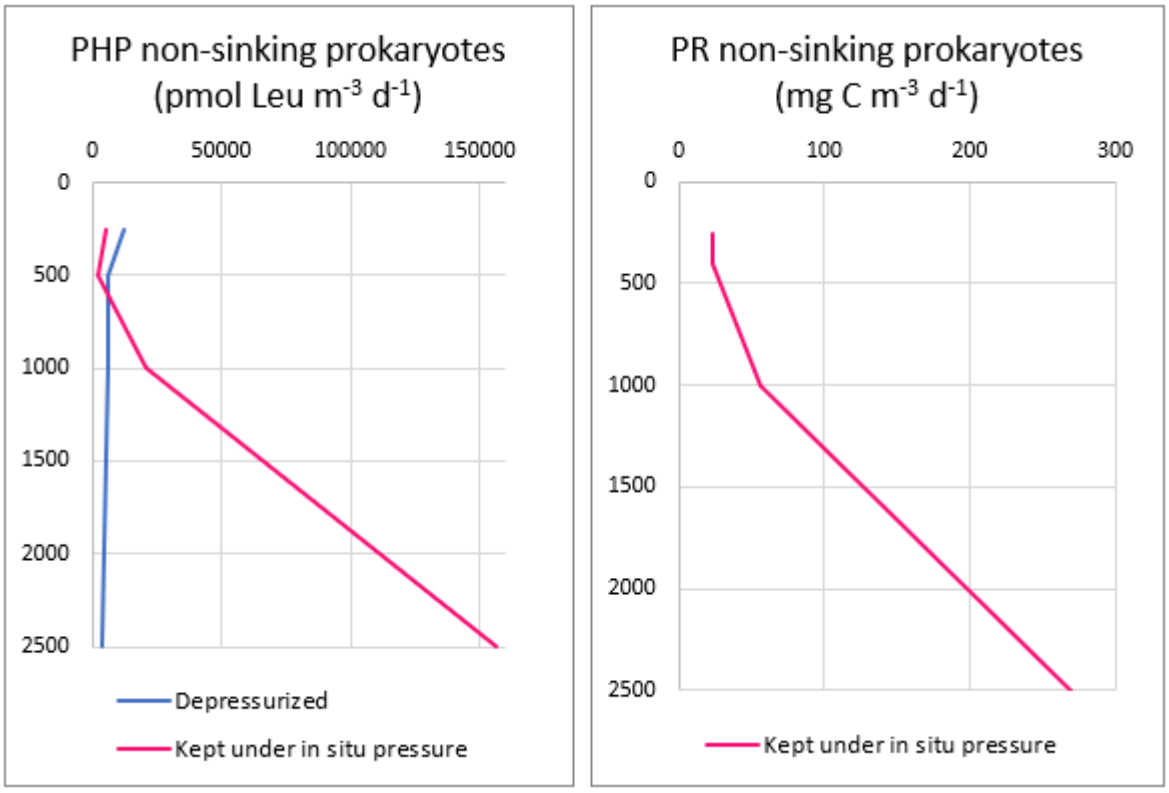

Figure S2: First plot of PHP and PR of non-sinking prokaryotes under in situ pressure compared to depressurized one. Data are from Peacetime cruise, Mediterranean sea.

SUPP DATA BIBLIOGRAPHY:

Boyd, P. W., A. McDonnell, J. Valdez, D. LeFevre, and M. P. Gall. 2015. RESPIRE: An in situ particle interceptor to conduct particle remineralization and microbial dynamics studies in the oceans' Twilight Zone. Limnology and Oceanography: Methods **13**: 494–508. doi:10.1002/lom3.10043

Burd, A. B., D. A. Hansell, D. K. Steinberg, and others. 2010. Assessing the apparent imbalance between geochemical and biochemical indicators of meso- and bathypelagic biological activity: What the @$#! is wrong with present calculations of carbon budgets? Deep-Sea Research Part II: Topical Studies in Oceanography 1557–1571. doi:10.1016/j.dsr2.2010.02.022

Collins, J. R., P. D. Fucile, G. McDonald, J. E. Ossolinski, R. G. Keil, J. R. Valdes, S. C. Doney, and B. A. S. Van Mooy. 2018. An autonomous, in situ light-dark bottle device for determining community respiration and net community production. Limnology and Oceanography: Methods **16**: 323–338. doi:10.1002/lom3.10247

del Giorgio, P. A., and J. J. Cole. 1998. BACTERIAL GROWTH EFFICIENCY IN NATURAL AQUATIC SYSTEMS. Annual Review of Ecology and Systematics **29**: 503–541. doi:10.1146/annurev.ecolsys.29.1.503

Hoppe, H.-G., H. Ducklow, and B. Karrasch. 1993. Evidence for dependency of bacterial growth on enzymatic hydrolysis of particulate organic matter in the mesopelagic ocean. Marine Ecology Progress Series **93**: 277–283.

Iversen, M. H., N. Nowald, H. Ploug, G. A. Jackson, and G. Fischer. 2010. High resolution profiles of vertical particulate organic matter export off Cape Blanc, Mauritania: Degradation processes and ballasting effects. Deep Sea Research Part I: Oceanographic Research Papers **57**: 771–784. doi:10.1016/j.dsr.2010.03.007

Langdon, C. 1984. Dissolved oxygen monitoring system using a pulsed electrode: design, performance, and evoluation. Deep Sea Research Part A. Oceanographic Research Papers **31**: 1357–1367. doi:10.1016/0198-0149(84)90006-2

Packard, T. T., M. Denis, M. Rodier, and P. Garfield. 1988. Deep-ocean metabolic CO2 production: calculations from ETS activity. Deep Sea Research Part A. Oceanographic Research Papers **35**: 371–382. doi:10.1016/0198-0149(88)90016-7

Ploug, H., and B. B. Jorgensen. 1999. A net-jet flow system for mass transfer and microsensor studies of sinking aggregates.

Robert, A. 2012. Minéralisation in situ de la matière organique le long de la colonne d'eau : application sur une station eulérienne. These de doctorat. Aix-Marseille.

Robinson, C. 2019. Microbial Respiration, the Engine of Ocean Deoxygenation. Frontiers in Marine Science **5**: 1–13. doi:10.3389/fmars.2018.00533

Tamburini, C., J. Garcin, and A. Bianchi. 2003. Role of deep-sea bacteria in organic matter mineralization and adaptation to hydrostatic pressure conditions in the NW Mediterranean Sea. Aquatic Microbial Ecology **32**: 209–218. doi:10.3354/ame032209

Tengberg, A., J. Hovdenes, H. J. Andersson, and others. 2006. Evaluation of a lifetime-based optode to measure oxygen in aquatic systems.doi:10.4319/lom.2006.4.7

Van Mooy, B. A. S., and R. G. Keil. 2015. Aquatic sample analysis system. patent n° US9188512B2

Van Wambeke, F., E. Pulido, P. Catala, and others. 2021. Spatial patterns of ectoenzymatic kinetics in relation to biogeochemical properties in the Mediterranean Sea and the concentration of the fluorogenic substrate used. Biogeosciences **18**: 2301–2323. doi:10.5194/bg-18-2301-2021